



In silico Investigation of the Antimalarial Activity of some Selected Alkaloids and Terpenoids Present in the Aerial Parts of *Andrographis paniculata*.

Oladapo J. Olaosebikan¹, Esther O. Faboro¹, Olatomide A. Fadare², Adebomi A. Ikotun^{1*}¹Chemistry Programme, College of Agriculture, Engineering and Science, Bowen University, Iwo, Osun State, Nigeria.²Department of Chemistry, Obafemi Awolowo University, Faculty of Science, Ile-ife, Osun State, Nigeria

ARTICLE INFO

ABSTRACT

Article history:

Received 05 May 2023

Revised 04 August 2023

Accepted 23 August 2023

Published online 01 September 2023

Copyright: © 2023 Wresdiyati *et al.* This is an open-access article distributed under the terms of the [Creative Commons Attribution License](https://creativecommons.org/licenses/by/4.0/), which permits unrestricted use, distribution, and reproduction in any medium, provided the original author and source are credited.

Most of the frontline drugs being used to treat malaria are gradually losing efficacy due to parasite resistance and this stipulates that new antimalarial drugs are discovered and developed either from plant origin or synthesis this study employed computational techniques to investigate the potential of phytochemicals from a medicinal plant (*Andrographis paniculata*) to act as potential inhibitors of *Plasmodium falciparum* Dihydroorotate Dehydrogenase (*Pf*DHODH). In this study, the aerial parts of *Andrographis paniculata* were locally sourced and processed, and cold extraction was carried out using 100 % dichloromethane, ethyl acetate and methanol. The extracts were characterized using GC-MS analysis to identify the various phytochemicals present. Spectra analysis revealed the presence of secondary metabolites, majorly alkaloids and terpenoids. The GC-MS revealed 60 compounds which were docked against *Pf*DHODH and screened using the known inhibitor, 5-methyl-7-(naphthalen-2-ylamino)-1H-{1,2,4}triazolo{1,5-a}pyrimidine-3,8-diiium, DSM1, as reference. 16 compounds were selected for druglikeness and in-silico pharmacokinetic property prediction and these were submitted to the online server, Admetlab 2.0. Based on the druglikeness assessment (Quantitative Estimate of Druglikeness, QED), 6 of the compounds were found to possess druglike qualities and these six were alkaloids and terpenoids, including Andrographolide. After considering other Pharmacokinetic parameters such as absorption, distribution, metabolism and toxicity, 4 compounds were eventually selected as potential *Pf*DHODH inhibitors with optimum pharmacokinetic properties that are worth considering as lead compounds for an antimalarial drug discovery effort. The four compounds identified are 6-methoxy-2-methyl-quinoline-3-carboxylic acid-2-dimethylamino-ethylester (MET24_671), Andrographolide (MET25_998), 1-(6-puriny)-2-pyrrolidinecarboxylic acid (DCM14_463) and 2-ethylacridine (EA24_614) of which DCM14_463 was deemed the best.

Keywords: Terpenoids, Alkaloids, Antimalarial, *Andrographis paniculata*, *In silico* studies

Introduction

Andrographis paniculata (Burm.f.) Nees, a member of the Acanthaceae family, is commonly called "Creat" or "King of Bitters" in English,¹ and it is mostly used in ancient oriental and Ayurvedic medicine.² It is commonly grown in South East Asia, Southern Asia, and China.³ Figure 1 presents the aerial parts of *A. paniculata*. Phytochemicals are plant chemicals that display great health benefits,⁴ which possess great antioxidant properties that fight several human diseases.⁴ Several synthetic compounds also possess antioxidant properties,⁵ but natural and organic compounds are most preferable. Phytochemicals in *A. paniculata* include alkaloids, terpenoids, flavonoids, phenols and tannins.⁶ These classes of compounds have shown remarkable health benefits, some of which are antioxidant, analgesic, anti-inflammatory, antidote for snakebite, antimalarial, antipyretic, and anticancer, amongst others.^{3,7}

*Corresponding author. E mail: adebomi.ikotun@bowen.edu.ng
Tel: +234 803 585 6562

Citation: Olaosebikan OJ, Faboro EO, Fadare OA, Ikotun AA. *In silico* Investigation of the Antimalarial Activity of some Selected Alkaloids and Terpenoids Present in the Aerial Parts of *Andrographis paniculata*. Trop J Nat Prod Res. 2023; 7(8):3787-3799 <http://www.doi.org/10.26538/tjnpr/v7i8.33>

Official Journal of Natural Product Research Group, Faculty of Pharmacy, University of Benin, Benin City, Nigeria

A. paniculata has been used to treat several diseases in traditional medicine across the globe, such as cold and fever, sore throat, sore tongue, and snake bite with excellent function of clearing heat and toxin, cooling blood and detumescence, and so on.⁸⁻¹⁰ It is also cultivated in Nigeria, where it is prominently used locally to treat malaria fever.⁶ The most studied phytochemical constituent of *A. paniculata* is Andrographolide A, which is a diterpene lactone that has been investigated for possible antimalarial, anti-inflammatory and anticancer activities.^{8,11}

It has become expedient to search for new and potent antimalarial agents apart from those that are currently being used clinically, considering that the parasite has developed resistance to the current frontline drugs and the resistant strain is spreading at an alarming rate across the globe.¹²⁻¹⁷ However, new potential antimalarial agents are expected to have a mechanism of action, affect different metabolic pathways and target proteins other than those that the current drugs affect since the parasite has already developed resistance by mutations that render the drugs that target such pathways ineffective. Sulfadoxine and pyrimethamine target folate synthesis (DHFR and DHPS),^{18,19} chloroquine and other quinine-based drugs target the biocrystallization of hemozoin,^{20,21} while the Artemisinin derivatives operate by a redox cycling process which generates free radicals that overwhelms the parasite.^{22,23} Therefore, new drug discovery approaches are looking for compounds that will potentially inhibit targets in other critical metabolic pathways in the parasite such as the Pentose phosphate pathway controlled by the transketolase enzyme^{24,25} or exploitation of the inability of the parasite to make purines (purine auxotroph) which it salvages from host erythrocytes by the help of parasite adenosine deaminase and purine nucleoside phosphorylase

(both proteins are also potential targets for drug discovery efforts,^{26,27} as well as pyrimidine synthesis, as a precursor for nucleobases used for building parasite DNA and RNA which is controlled by Dihydroorotate dehydrogenase (DHODH) that has been selected as target for this study.^{28,29}

In the synthesis of Deoxyribonucleic acid and Ribonucleic acid, pyrimidines serve as necessary precursor metabolites.³⁰ A cell can obtain pyrimidine either by the salvage pathway that uses pyrimidine bases (such as cytosine and thymine) or nucleosides acid (such as uridine and cytidine), or through the *de novo* syntheses pathway, using ammonia (produced from L-glutamine), bicarbonate, and L-aspartic acid. The *de novo* synthesis pathway is the only source of pyrimidines for cell growth, but *Plasmodium* species lack the salvage enzymes.³¹ Stage 4 in the pyrimidine *de novo* synthesis pathway is catalyzed by a flavin mononucleotide-dependent enzyme known as dihydroorotate dehydrogenase (DHODH), which converts dihydroorotate to orotic acid. *Plasmodium falciparum* Dihydroorotate Dehydrogenase (*Pf*DHODH) has emerged as a promising target for the malaria drug discovery effort because of the necessity of pyrimidines in cell growth, metabolism, and replication. Furthermore, due to the vital involvement of *Pf*DHODH in the *de novo* synthesis of pyrimidine and its druggability, which far outweighs that of other enzymes in the pathway, it is being considered a target for malaria drug discovery by many research groups across the globe.³² Figure 2 presents the synthesis of Pyrimidine nucleotides via the *de novo* synthesis pathway.³¹

This study used computational techniques to investigate the antimalarial potential of selected phytochemicals (of the classes, terpenoids and alkaloids) found in the various extracts of the aerial parts of *A. paniculata*, such as molecular docking and Pharmacokinetics property predictions. Essentially, determining the binding affinity of the selected phytochemicals for the target protein (DHODH) as an estimate for the potential to inhibit the target protein as well prediction and analysis of druglikeness and pharmacokinetics properties (Absorption, Distribution, Metabolism, Excretion and Toxicity) as filters to aid the identification of likely phytochemicals that may be responsible for the antimalarial activity observed for the study plant (*A. paniculata*).



Figure 1: The aerial parts of *Andrographis paniculata*

Materials and Methods

Experimental

Sample collection

The aerial parts of *A. paniculata* were obtained in October 2021, from the National Institute of Horticulture (NIHORT), Ibadan, Oyo state, Nigeria (7° 25' N, 3° 52' E). It was authenticated at the Plant Biology Programme of the College of Agriculture, Engineering and Science, Bowen University, Iwo, Osun state, where it was given the Herbarium number BUH031.

Sample processing

The aerial parts were thoroughly rinsed using water and air-dried in a well-ventilated area at room temperature of 29 °C for two weeks. The dried sample were pounded using a locally made mortar and pestle (to reduce the size of the twigs and leaves) and later pulverized into a coarse powder, using an electrical blender (Heavy Duty 750 watt

Solaire Mixer-Grinder, India), the product was weighed and stored in an air-tight container for further processing.

Extraction

The extraction process was carried out using the sequential order of dichloromethane, ethyl acetate and methanol (100 % concentration of the solvents were used) according to Faboro *et al.*, 2016³³ (with some modifications). 250 g of the ground sample was soaked with 750 mL of dichloromethane for 24 hours with constant stirring. After extraction with methanol, the marc was dried and then soaked in 750 mL of ethyl acetate for 24 hours with constant stirring. Similarly, after extraction with ethyl acetate, the marc was dried and then soaked with 750 mL of methanol for 24 hours with constant stirring.

Concentration

The solvent from each extraction process was decanted and filtered using Whatman No.1 filter paper. The resulting filtrate was further concentrated using a rotary evaporator to remove the remaining solvent. In each case, a slurry was obtained; this was weighed and transferred into an air-tight container for further processing.

Characterization

The crude extracts were characterized using the Gas Chromatography-Mass Spectrometry technique (GC-MS, Agilent Technologies, United States). Here, an 8860A Gas Chromatograph coupled to a 5977C inert Mass Spectrometer with an electron impact source. For the separation of the compounds, an HP-5 capillary column coated with 5 % of Phenyl Methyl Siloxane (30 m × 0.32 mm × 0.25 µm film thickness), was the stationary phase and the carrier gas was helium, at a constant flow rate of 1.573 mL per minute, and the compounds were identified by comparing measured mass spectral data with those in "National Institute of Standard and Technology" (NIST) 14 Mass Spectral Library. Figures 3(i-iii), showed the Chromatogram of the GC-MS analyses of the dichloromethane, ethyl acetate and methanol extracts respectively, while Table 1 and 2 showed the GC-MS data table for the selected study compounds (the major compounds and those that appear as trace).

In Silico studies

All the compounds identified from the extracts of *A. paniculata* (aerial parts) were studied, the compound profile from the GC-MS puts the compounds identified into two broad categories, i.e alkaloids and terpenoids. The reference ligand (inhibitor of *Pf*DHODH that bound to the crystal structure of the target enzyme) is code-named DSM1 (5-methyl-N-naphthalen-2-yl-1,2,4-triazolo{1,5-a}pyrimidin-7-amine), with PDB ID: 3I65.

Preparation of selected phytochemicals for Molecular Docking

The 3D conformer structures of the identified compounds were downloaded from ChemSpider (Chemspider.com) in .sdf formats and converted to their .pdb formats using Open Babel,³⁴ and each of the ligands was loaded into AutoDockTools, where they were further processed and saved in .pdbqt format, for docking using AutoDock Vina.³⁵

Receptor preparation

The 3D conformer of the enzyme was downloaded from the Protein Data Bank (<https://www.rcsb.org>) and loaded to PyMOL-v1.74 software for pre-docking analyses (such as removal of water molecules and determining the active site),³⁶ the processed enzyme was then saved in the .pdb format for docking activity. The active site of the receptor was determined by identifying the amino acid residues within 4 Å of the known inhibitor bound to the receptor.³⁷

Molecular Docking

The Molecular docking was carried out using the AutoDock Vina software.³⁵ The search space area was set around the active site with a grid box of size (x = 56, y = 38, z = 44), and centre (x = -4.315, y = 29.483 and z = 14.129), and these were used for the molecular docking. The post-docking studies were done using PyMOL-v1.74

software.³⁶ The inhibitor of the target enzyme (DSM1) was used as the reference.

The method adopted for the molecular docking was validated by redocking the native ligand of the downloaded protein into the protein and the docking output superimposed over the undocked ligand and the rmsd evaluated using the command line of PyMOL.

ADMET properties

The ADMET properties of the study compounds (ligands) and the reference ligand were predicted using the online server, ADMETlab 2.0. Here the Canonical SMILES of the compounds were loaded to the ADMETlab 2.0 server.³⁸

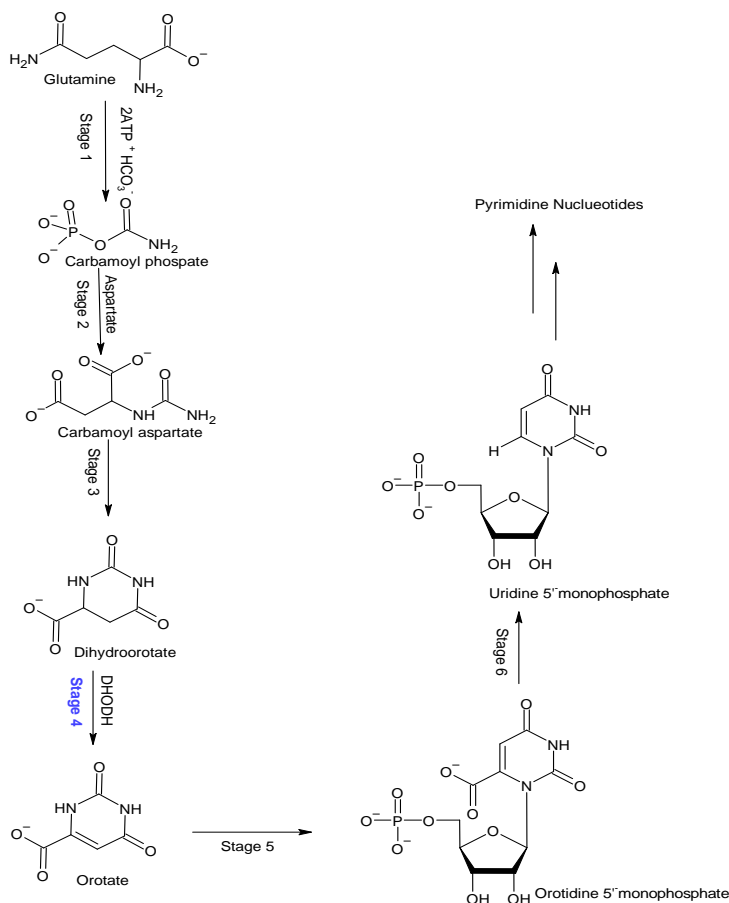


Figure 2: Synthesis of pyrimidine nucleotides via the *de novo* synthesis pathway, DHODH is very important in stage 4 as it catalyzes the conversion of dihydroorotate to orotate.

Results and Discussion

Compound Identification from GC-MS

The chromatogram for the extracts is presented in Figures 3(i-iii) and the compounds identified based on their mass spectra and matching with appropriate references in the NIST library are presented in Tables 1 and 2. The printout of the Library report and other metadata are submitted as supplementary material.

Molecular Docking

The docking protocol was deemed accurate and appropriate after redocking the native ligand and obtaining an rmsd of 0.15 Å for the superimposed docked and native ligand (Figure 4). The compounds identified (60 compounds), based on the names given from the NIST library report and library matching of Mass spectra, were docked against the receptor, and their binding affinity was estimated in kcal/mol. The binding affinity of the reference ligand was also estimated for comparison, as a measure of the potential for inhibition of the enzyme by the study compounds relative to that of the reference ligand. The corresponding binding affinity values of the study compounds are recorded in the table (Tables 1 and 2) for each compound. The binding affinity of the reference compound, DSM1, was estimated to be -12.3 kcal/mol (Figure 4) and used as a benchmark for screening potential inhibitors from among the 60 compounds docked.

The compounds that have a binding affinity of -8.0 kcal/mol (at least 65 % of the energy of the reference compound) and above were selected for in-silico pharmacokinetic property prediction. Table 3 shows the binding affinities and structures of the compounds with relatively higher binding affinity selected for further screening. The alkaloids, though present as trace and minor components of the extracts, are among the compounds that have been predicted to have a high binding affinity for the target protein relative to DSM1. It is possible that irrespective of the very low amount of the alkaloids in the extracts, their presence will contribute much to any biological activity particularly the inhibition of *Pj*DHODH. And these alkaloids can be explored further (individually) as potential *Pj*DHODH inhibitors.

The terpenoids among the selected compounds however appear to be more prominent in the extracts when compared to the alkaloids and also have among them, compounds with the highest estimated binding affinity such as squalene and phytol (that showed up in multiple extracts – Table 1) including long chain fatty acids.

Table 1: Table showing the binding affinity of the prominent/major components of the plant extracts

S/N	Compounds (Coded with retention time)	IUPAC Name of compounds	Binding Energy (-kcal/mol)
1	DSM1 (Reference ligand)		12.3
2	DCM19_034*	Neophytadiene	7.8
3	DCM19_469**	3,7,11,15-Tetramethylhexadec-2-en-1-ol	8
4	DCM20_276†	Hexadecanoic acid	7.2
5	DCM21_695***	Phytol	8
6	DCM27_669****	squalene	10
7	DCM27_869	1H-cycloprop[e]azulene	8.1
8	DCM28_979	Sitosterol	6.2
9	EA19_023*	Neophytadiene	7.8
10	EA19_281	3,7-dimethyloct-6-en-1-yl-3-methylbutanoate	7.6
11	EA19_464**	3,7,11,15-Tetramethylhexadec-2-en-1-ol	8.1
12	EA20_271†	Hexadecanoic acid	6.9

13	EA20_311	Diisopropyl phthalate	7.8
14	EA21_684**	3,7,11,15-Tetramethylhexadec-2-en-1-ol	8.1
15	EA21_930	9,12,15-octadecatrien-1-ol	7.7
16	EA22_622*	Neophytadiene	8.1
17	EA27_663****	Squalene	10.2
18	EA27_847	Cycloheptane-4-methylene-1-methyl-2-(2-methyl-1-propen-1-yl)-1-vinyl	5.8
19	EA28_682	(1E,3Z,6E,10Z)-12-isopropyl-1,5,9-trimethylcyclotetradeca-1,3,6,10-tetraene	5.6
20	MET11_585	Phenylethylamine, alpha-ethyl	6.5
21	MET12_883	2-methoxy-4-vinylphenol	6.8
22	MET13_387	Phenol-2,6-dimethoxy	6.1
23	MET15_727	2(4H)-Benzofuranone-5,6,7,7a-tetrahydro-4,4,7a-trimethyl	7.4
24	MET18_148	4-((1E)-3-hydroxy-1-propenyl)-2-methoxyphenol	7.3
25	MET18_674	2-cyclohexen-1-one-4-hydroxy-3,5,5-trimethyl-4-(3-oxo-1-butenyl)	7.1
26	MET19_023*	Neophytadiene	7.8
27	MET19_458	Tetradec-13-en-11-yn-1-ol	6.8
28	MET19_910	Hexadecanoic acid, methyl ester	7.1
29	MET20_396†	Hexadecanoic acid	7.1
30	MET21_089	Cis-p-mentha-1(7),8-dien-2-ol	6.3
31	MET21_529	9,12-octadecadecanoic acid, methyl ester	7.7
32	MET21_598	9,12,15-octadecatrienoic acid, methyl ester	8.2
33	MET21_701***	Phytol	8.1
34	MET22_050	(9Z,12Z,15Z)-octadeca-9,12,15-trienoic acid	8
35	MET22_182	Octadecanoic acid	7.2
36	MET23_566	methyl parinarate	8.6
37	MET24_047	1-(phenylethynyl)-1-cyclopentanol	7.9
38	MET24_671	6-methoxy-2-methyl-quinoline-3-carboxylic acid-2-dimethylamino-ethylester	8.1
39	MET25_048	Hexadecanoic acid-2-hydroxyl-1-(hydroxymethyl)ethyl ester	7.4
40	MET25_300	2-amino-4-morpholino-6-phenylcarbamoyl-1,3,5-triazine	8.3
41	MET25_998	Andrographolide	8.5
42	MET26_502	(6Z,9Z,12Z,15Z)-Methyl octadeca-6,9,12,15-tetraenoate	8.1
43	MET26_645	octadecanoic acid-2,3-dihydroxypropyl ester	7.7
44	MET27_669****	Squalene	10.4
45	MET27_915	1(2H)-Naphthalenone-3,4,4a,5,8,8a-hexahydro-8a-methyl	6.3
46	MET5_285	Glycine-N,N-dimethyl-,methylester	4.6

* Neophytadiene, appearing multiple times in different solvents; ** 3,7,11,15-Tetramethylhexadec-2-en-1-ol, appearing multiple times in different solvents

*** Phytol, appearing multiple times in different solvents; **** Squalene, appearing multiple times in different solvents; † Hexadecanoic acid, appearing multiple times in different solvents

Table 2: Table showing the binding affinity of the trace components of the plant extracts

Serial Number	Compounds (Coded with retention time)	IUPAC Name of compounds	Binding Energy (-kcal/mol)
1	DSM1 (Reference ligand)		12.3
2	DCM14_463	1-(6-puriny)-2-pyrrolidinecarboxylic acid	8.2
3	DCM14_897	(4Z)-5-chloro-3,4-dimethyl-2,4-heptadiene	6
4	DCM15_138	2-ethyl-6-methylphenyl isothiocyanate	6.1
5	DCM15_739	2(4H)-Benzofuranone-5,6,7,7a-tetrahydro-4,4,7a-trimethyl	6.7
6	DCM17_026	4-methylphenol, n-propylether	6.5
7	DCM18_422	5-caranol	5.9
8	EA15_733	2(4H)-Benzofuranone-5,6,7,7a-tetrahydro-4,4,7a-trimethyl	7.4
9	EA17_015	1H-indene-2,3-dihydro-1,1,5,6-tetramethyl	7.1
10	EA24_614	2-ethylacridine	9.3
11	EA25_295	1-methyl-4-phenyl-5-thioxo-1,2,4-triazolidin-3-one	6.7
12	MET11_167	Hexacosylamine-N,N-dimethyl	8.1
13	MET13_810	2-propenoic acid, 3-phenyl-methylester	7
14	MET15_229	5-cyclopropyl-2H-pyrazole-3-carbaldehyde	6.2
15	MET15_579	1-(2-ethoxyphenyl)acetone	7
16	MET15_727	2(4H)-Benzofuranone-5,6,7,7a-tetrahydro-4,4,7a-trimethyl	7.4
17	MET16_076	2,3,5,6-tetrafluoroanisole	6.4
18	MET16_820	Benzen-1,3-diethyl-5-methyl	7.1
19	MET17_295	1,8-Nonadiene-2,7-dimethyl-5-(1-methylethenyl)	6.5
20	MET19_092	2-pentadecanone-6,10,14-trimethyl	7.7
21	MET19_281	2-methyl-3-(3-methyl-but-2-enyl)-2-(4-methyl-pent-3-enyl)-oxetane	7
22	MET25_741	Ethanone-1-(4-hydroxy-3,5-dimethoxyphenyl)	6.7
23	MET27_160	Thunbergol	5.8
24	MET28_487	1,1,4,7-Tetramethyldecahydro-1H-cyclopropa[e]azulene-4,7-diol	6.2
25	MET28_688	Androstan-17-one-3-ethyl-3-hydroxyl-,(5.alpha.)	8.4

There appear to be two binding sites in the *PfDHODH*, one is the inhibitor binding site (which is an allosteric site) – the site to which DSM1 was bound in the crystal structure of *PfDHODH*. The other site is the active site of the protein where the co-factor and substrate are bound (Figure 5). Both sites are connected by a narrow groove. It is worth noting that a similar study of alkaloids from *Cryptolepis sanguinolenta* executed by Kyei *et al.*, 2022³⁹ made similar observations, whereby they concluded that there were two domains in the protein that ligands can bind to, which they described as the inhibitor binding domain, and another, described as the flavin mononucleotide (FMN) binding domain – the site that the co-factor and substrate occupy, which is also the active site some of the study compounds (MET24_671, MET25_998, MET28_688) docked into the active site (FMN binding domain). A few compounds also bound to the allosteric site (inhibitor binding domain), DCM27_869, EA24_614, MET25_300, and MET26_502. The compounds that

bound to the active site and allosteric site are majorly alkaloids and terpenoids.

The compounds that bound to the inhibitor binding domain had extensive hydrophobic interaction, plenty of Pi-Pi and Pi-alkyl interactions and few polar interactions with the enzyme, only the PUFA (MET26_502) with its oxygenated end and an alkaloid, MET25_300 with one polar interaction as well (Figure 6). The high binding affinity for the protein at the allosteric site may be an indication that strong binding at that site may elicit inhibition (irrespective of the lack of polar interactions by the compounds). This might mean the binding to the allosteric site is critical for the inhibition of the enzyme which was also observed in the study by Kyei *et al.*, 2022.³⁹ An analysis of the residues at the active site reveals that there is a high population of non-polar (hydrophobic) residues, LEU, PHE, GLY, MET and VAL essentially with a few polar residues such as CYS, HIS and ARG, which sets up the inhibitor binding domain in

such a way that it prefers rigid hydrophobic entities that can be held in place by extensive Van der Waals interactions with LEU (majorly), PHE, GLY, MET and VAL and secured by a few polar interactions with HIS or ARG spangled in between the non-polar residues. This may be the reason why DSM1, with its triazolopyrimidine ring system, joined to a naphthyl ring by an sp^3 hybridized -NH-, has a very high affinity for the active site (being essentially non-polar with a hydrogen bond donor and a couple of hydrogen bond acceptors). The hydrophobic naphthyl ring fused to the nitrogen heterocycle appears to fit properly in the allosteric site with many nitrogen atoms that can be used for tethering at the inhibitor binding domain.

Thus, it is no surprise if fused heterocycles, some of the alkaloids (EA24_614, an acridine-based compound and MET25_300, a triazine) and an azulene derivative, DCM27_869) in this study have a high affinity for the allosteric site. EA24_614, the acridine alkaloid has the highest binding affinity (-9.3 kcal/mol) for the protein at the inhibitor binding domain but without polar interactions. And our findings agree with those of Kyei *et al.*, 2022,³⁹ as they concluded that “hydrophobic interactions drive ligand binding to the inhibitor binding domain and hydrogen bonding provides quinone specificity”. Kyei *et al.*, 2022,³⁹ also concluded that all alkaloids of the aromatic and planar group among the class of studied compounds may be strong *Pf*DHODH inhibitors exploiting full hydrophobic advantages in contrast to those of the class that consists of sterically bulky groups.³⁹ The alkaloids observed to be likely potent inhibitors of the *Pf*DHODH in this study have similar structural features with those observed to be likely potent inhibitors by Kyei *et al.*, 2022.³⁹

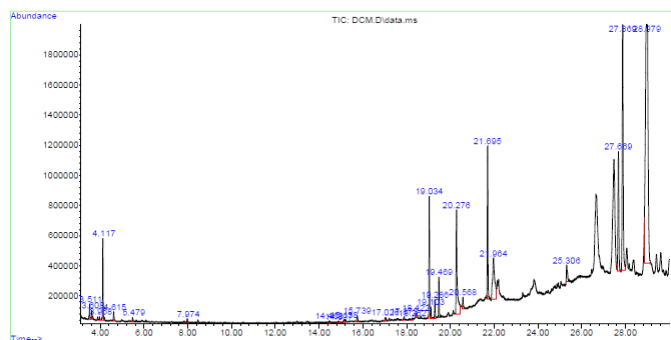


Figure 3(i): Chromatogram of Dichloromethane extract

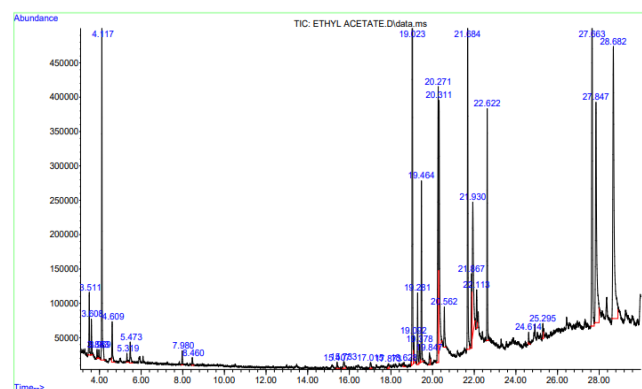


Figure 3(ii): Chromatogram of Ethyl Acetate extract

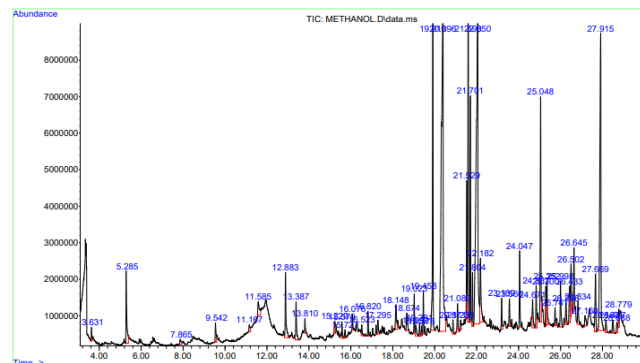


Figure 3 (iii): Chromatogram of Methanol extract

The 2D diagrams (Figure 6) of the interactions of the docked compounds (particularly those that bound to the inhibitor binding domain) in this study also show extensive hydrophobic interactions (mostly Pi=Pi and Pi-alkyl) which might have contributed to the high binding affinity estimated for the compounds. Three other alkaloids bound to the active site and have a high binding affinity, API24_968 (an indole alkaloid), MET24_671 (a quinoline alkaloid) and DCM14_463 (a purine alkaloid) and with extensive polar interactions (Figure 6) which also make them potential inhibitors of *Pf*DHODH that may be considered for further exploration (lead compounds).

The terpenoids, andrographolide and 3-ethyl-3-hydroxy-androstan-17-one also featured as *Pf*DHODH active site binders with high binding affinity. Andrographolide is well known for some potent pharmacological activity and has been investigated for potential antimalaria activity recently⁴⁰.

It was also observed in this study that some long-chain hydrocarbons can extend through the narrow groove that connects the two binding domains and therefore partly occupy both binding domains. These include DCM27_669 (squalene), EA19_464 (phytol), EA22_622 (Neophthadiene), MET21_598 (FFA), MET22_050 (FFA), MET23_566 (FFA) and MET11_167 (Hexacosylamine-N,N-dimethyl). Squalene has a very high binding affinity (-10 kcal/mol) while all the other groove binders have a binding affinity that is centred around -8.1 kcal/mol. These groove binders have not been considered in previous literature for *Pf*DHODH inhibition and these compounds are also good candidates for a future in-vitro and in-vivo investigation, particularly squalene and phytol, that are already known to possess some pharmacological activity⁴¹⁻⁴³. It is believed, however, that because of the oily (high lipophilicity) nature of the squalene and phytol, they may not perform well in in-vitro studies (the low water solubility of the squalene and phytol may prevent them from reaching the target protein in in-vitro experiments in which the medium is essentially aqueous) but may still contribute to observed activity for the extracts in in-vivo experiments.

Based on the estimates of the binding affinity of the native ligand (DSM1) relative to the other study compounds, the DSM1 is expected to be more potent as a *Pf*DHODH inhibitor however, if the extract of the plant is used as a therapy for malaria (considering that the *Pf*DHODH may be a likely target), the extract may perform better because of the cocktail of compounds present that have high binding affinity (comparable to that of DSM1) for the target protein. The cocktail of compounds may work synergistically.

ADMET properties

The ADMET properties of the selected study compounds are presented in Table 4. The druglikeness of the compounds was predicted as Quantitative Estimate of Druglikeness (QED), A measure of drug-likeness based on the concept of desirability. According to the Admet lab 2.0 program,³⁸ QED is a metric used in drug discovery and medicinal chemistry to estimate the drug-likeness of chemical compounds. It evaluates how similar a molecule is to known drugs and how likely it is to possess favorable pharmacological properties.

The QED score is calculated based on eight drug-likeness-related properties of a molecule:

MW (Molecular Weight): The molecular weight of the compound.

log P (Octanol-Water Partition Coefficient): A measure of the lipophilicity of the compound, which relates to its ability to pass through cell membranes.

NHBA (Number of Hydrogen Bond Acceptors): The count of hydrogen bond acceptor groups in the molecule.

NHBD (Number of Hydrogen Bond Donors): The count of hydrogen bond donor groups in the molecule.

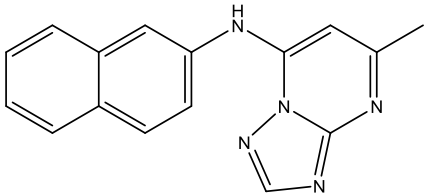
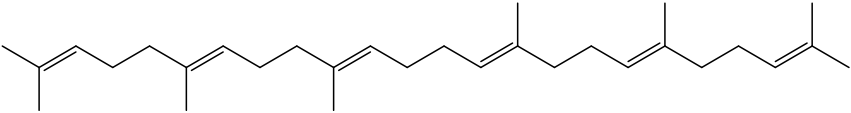
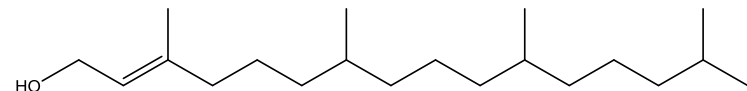
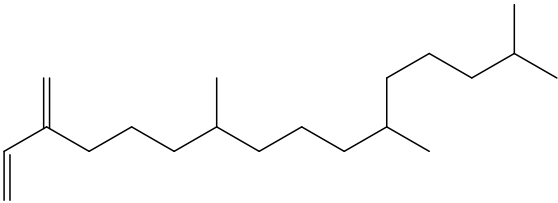
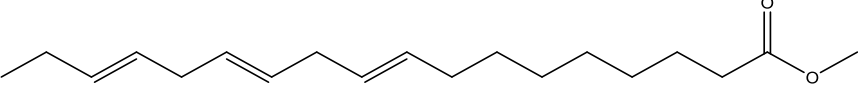
PSA (Polar Surface Area): The surface area of the molecule that is polar and capable of forming hydrogen bonds.

Nrotb (Number of Rotatable Bonds): The number of bonds that can freely rotate in the molecule.

NAr (Number of Aromatic Rings): The count of aromatic rings present in the molecule.

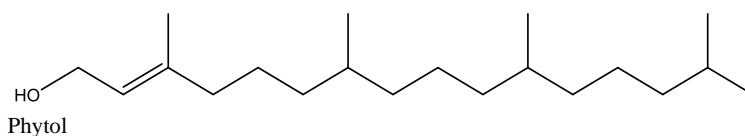
Table 3: Table of compounds (structures) with relatively higher binding affinity selected for pharmacokinetic predictions

(a) Compounds that are prominent/major constituents of extracts

S/N	Ligand	Structure	Binding affinity (-kcal/mol)
DSM1			12.3
DCM27_669	5-Methyl-N-(2-naphthyl)[1,2,4]triazolo[1,5-a]pyrimidin-7-amine		10
DCM27_869	Squalene		8.1
EA19_464	3,7,11,15-Tetramethylhexadec-2-en-1-ol		8.1
EA22_622	Neophytadiene		8.1
MET21_598	9,12,15-octadecatrienoic acid, methyl ester		8.2

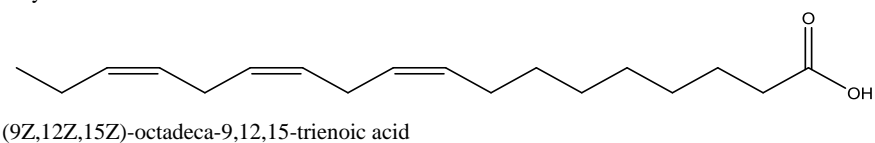
MET21_701

8.1



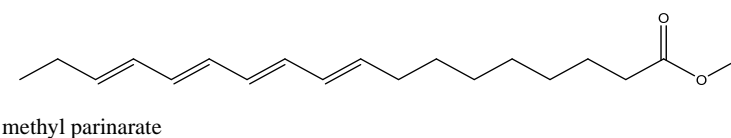
MET22_050

8



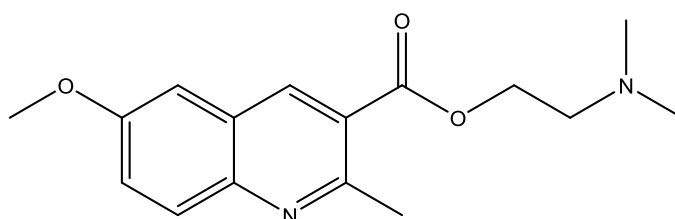
MET23_566

8.6



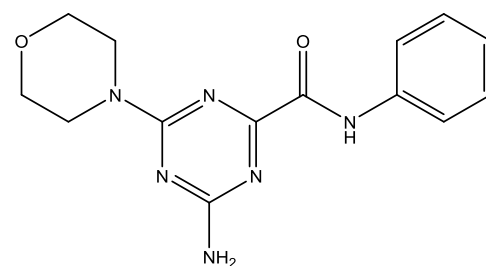
MET24_671

8.1



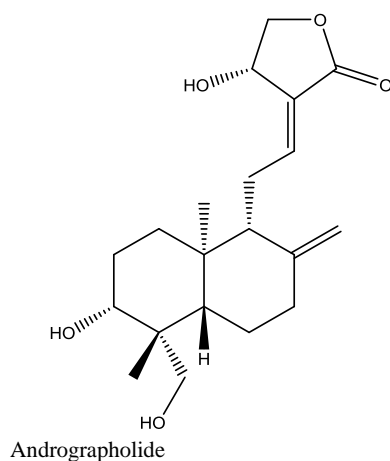
MET25_300

8.3

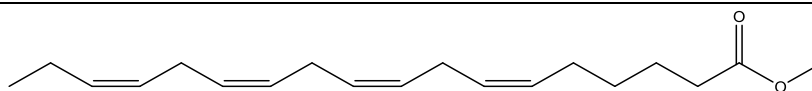


MET25_998

8.5



MET26_502



(6Z,9Z,12Z,15Z)-Methyl octadeca-6,9,12,15-tetraenoate

8.1

(b) Compounds that are trace constituents of extracts

S/N	Ligand	Structure	Binding affinity (-kcal/mol)
DCM14_463	(Alkaloid)	 1-(6-purinyl)-2-pyrrolidinecarboxylic acid	8.2
DSM1		 5-Methyl-N-(2-naphthyl)[1,2,4]triazolo[1,5-a]pyrimidin-7-amine,	12.3
EA24_614	(Alkaloid)	 2-ethylacridine	9.3
MET11_167	(wax)	 Hexacosylamine-N,N-dimethyl	8.1
MET28_688	(Terpenoid)	 Androstan-17-one-3-ethyl-3-hydroxyl-,(5.alpha.)	8.4

Table 4: Table showing the predicted pharmacokinetic properties of selected compounds

S/N	Compounds (major components)	HIA	Caco-2	MDCK	PPB	CYP 3A4-inh	CYP 3A4-sub	hERG	Ames	Carcinogenicity	QED
1	DCM27_669.pdb	0.548	-4.912	0.0000093	95.56%	0.543	0.097	0.009	0	0.007	0.186
2	DCM27_869.pdb	0.003	-4.435	0.0000299	94.72%	0.16	0.309	0.035	0.831	0.719	0.45
3	EA19_464.pdb	0.004	-4.46	0.0000129	97.90%	0.189	0.105	0.014	0.002	0.033	0.392
4	EA22_622.pdb	0.002	-4.648	0.000006	98.16%	0.368	0.163	0.009	0.019	0.12	0.313
5	MET21_598.pdb	0.083	-4.832	0.0000407	100.05%	0.849	0.09	0.082	0.002	0.07	0.245
6	MET21_701.pdb	0.003	-4.513	0.0000125	98.99%	0.262	0.116	0.01	0.001	0.021	0.392
7	MET22_050.pdb	0.026	-5.191	0.0000804	98.89%	0.072	0.057	0.021	0.758	0.672	0.348
8	MET23_566.pdb	0.012	-4.392	0.0000349	97.17%	0.962	0.208	0.467	0.092	0.153	0.268
9	MET24_671.pdb**	0.004	-4.783	0.0000138	74.81%	0.023	0.594	0.729	0.1	0.221	0.79
10	MET25_300.pdb	0.499	-5.592	0.0000075	61.02%	0.016	0.229	0.065	0.059	0.906	0.759
11	MET25_998.pdb**	0.019	-4.818	0.0000285	36.142%	0.56	0.188	0.02	0.719	0.032	0.534
12	MET26_502.pdb	0.031	-4.929	0.0001376	98.28%	0.903	0.176	0.077	0.965	0.853	0.268
S/N	Compounds (trace components)	HIA	Caco-2	MDCK	PPB	CYP 3A4-inh	CYP 3A4-sub	hERG	Ames	Carcinogenicity	QED
13	DCM14_463.pdb**	0.017	-5.768	0.000005	26.09%	0.032	0.074	0.015	0.031	0.112	0.779
14	EA24_614.pdb**	0.003	-4.689	0.0000145	96.80%	0.593	0.245	0.443	0.84	0.696	0.55
15	MET11_167.pdb	0.005	-5.121	0.0000037	97.83%	0.166	0.049	0.99	0.008	0.025	0.136
16	MET28_688.pdb	0.005	-4.644	0.0000188	89.75%	0.95	0.709	0.544	0.012	0.719	0.758

HIA; Empirical decision: 0-0.3: excellent ; 0.3-0.7: medium ; 0.7-1.0: poor

Caco-2; Empirical decision: > -5.15: excellent ; otherwise: poor MDCK; Empirical decision: >2 x 10⁻⁶cm/s: excellent , otherwise: poor

PPB; Empirical decision: ≤ 90%: excellent ; otherwise: poor .

CYP3A4-inh; Category 0: Non-inhibitor; Category 1: inhibitor. The output value is the probability of being inhibitor, within the range of 0 to 1.

CYP3A4-sub; Category 0: Non-substrate; Category 1: substrate. The output value is the probability of being substrate, within the range of 0 to 1.

hERG; Empirical decision: 0-0.3: excellent ; 0.3-0.7: medium ; 0.7-1.0: poor

Ames; Empirical decision: 0-0.3: excellent ; 0.3-0.7: medium ; 0.7-1.0: poor

Carcinogenicity; Empirical decision: 0-0.3: excellent ; 0.3-0.7: medium ; 0.7-1.0: poor

QED; Empirical decision: > 0.67: excellent ; ≤ 0.67: poor

**Compounds with optimum pharmacokinetics (without toxicity considerations)

Number of alerts for undesirable functional groups: This indicates the presence of specific chemical features that may lead to undesirable pharmacological effects.

Each of these properties has an associated "desirability function" (di), which quantifies how desirable a specific value of that property is for drug-likeness. For example, a smaller molecular weight may be more desirable, while too many rotatable bonds might be less desirable.⁴⁴

The QED score for a molecule is calculated as the geometric mean of the individual desirability functions (d1 to d8) for the eight properties. A high QED score indicates a molecule with drug-like properties, while a lower score suggests a less drug-like compound.⁴⁴

$$QED = \exp[(1/n) * \sum (\ln(di))]$$

Where:

n = 8 (number of drug-likeness properties)

$\sum (\ln(di))$ is the sum of natural logarithms of the desirability functions for all eight properties.

After calculating the QED score for a compound, it falls into one of the following categories⁴³ based on its score:

Excellent: QED > 0.67 (rows highlighted as yellow).

Poor: QED ≤ 0.67.

So, compounds with QED scores greater than 0.67 are considered excellent, while those with scores equal to or less than 0.67 are considered poor while compounds with QED ≤ 0.34 are unattractive and too complex. Essentially, Compounds with QED scores between 0.34 and 0.67 are likely to be considered unattractive but not necessarily too complex, thus taking a score of 0.49 as midway between 0.67 and 0.34, compounds with scores around 0.49 were considered along those highlighted as yellow and these other set were given blue highlight for the row they occupy in Table 4.

It is interesting to note that almost all components in the trace category among the compounds selected based on binding affinity happen to pass the druglikeness assessment and among the components classified as major/prominent, the polar extract (methanol extract) presented the compounds that are also found to be druglike, MET24_671, MET25_300 and MET25_998. Essentially, the compounds being considered further are alkaloids except for the Androstane (MET28_688) and Andrographolide (MET25_998).

Based on the values predicted for Plasma Protein Binding, PPB, EA24_614 was eliminated. plasma protein binding (PPB) is a crucial process that influences the pharmacokinetics and by extension the pharmacodynamics of drugs. When a drug is administered into the bloodstream, it can exist in two forms: bound to plasma proteins or in its free (unbound) form. PPB refers to the extent to which a drug binds to proteins present in the plasma, such as albumin and alpha-1-acid glycoprotein. Understanding the extent of PPB helps to predict the drug's distribution, clearance, and pharmacological activity. It also plays a significant role in drug-drug interactions and can affect the overall efficacy and safety of drugs. According to the scoring for PPB on the ADMETlab 2.0 programme,³⁸ a compound is considered to have a proper PPB if it has a predicted value <90 % and drugs that are high protein-bound may have a low therapeutic index. Thus, EA24_614, having a PPB score of 96.80 % will be unsuitable because it tends to be poorly distributed and therefore eliminated from the pool of compounds being considered.

By virtue of the fact that the herbal preparations are administered orally, it is expedient that the compounds from the extracts are properly absorbed in the gastrointestinal tract to foster oral bioavailability, thus based on the assessment of cell permeability

scores and human intestinal absorption, component MET25_300 was eliminated from the pool of compounds being considered. The HIA score of 0.499 suggests that component MET25_300 will be poorly absorbed in the intestine (score of 0-0.3 considered as excellent; 0.3-0.7 considered as excellent)³⁷ relative to all other compounds found to be druglike. The remaining compounds in the pool have a low tendency to be metabolized by CYP3A4, the prominent CYP450 enzyme that metabolizes most xenobiotics, (except MET28_688) and their toxicity profile were considered. Among the remaining four compounds, MET24_671 had a score closest to 1.0 and the highest potential to be an hERG inhibitor and elicit cardiotoxicity, meanwhile according to the Ames test for mutagenicity, MET25_998 and MET28_688 have scores close to 1.0 which indicates a greater potential to be mutagenic. The assessment of the toxicity profile for the remaining four compounds leaves DCM14_463 as the compound with optimum pharmacokinetics among the seven found to be druglike in the first instance. DCM14_463 is an alkaloid and unfortunately, present in trace amounts in the study plant.

Conclusion

Four compounds (MET24_671, MET25_998, DCM14_463, EA24_614) have been identified from this study as potential *Pf*DHODH inhibitors that also have optimum pharmacokinetic properties that may end up being useful drugs for treating malaria. Three of the four are alkaloids and one is a terpenoid, andrographolide, a well-known sesquiterpene lactone from *Andrographis paniculata* that has been investigated widely for its potential pharmacological activities. And DCM14_463 stands out from among the lot as being the component with the least potential for toxicity although present in trace amounts in the plant extract. These compounds could be purchased or isolated and tested individually in an *in-vitro* inhibitory experiment to assess their inhibitory potential of the *Pf*DHODH. The compounds could also be combined to study their synergistic effect since they usually occur together in the plant as a mixture of phytochemicals.

Conflict of Interest

The authors declare no conflict of interest.

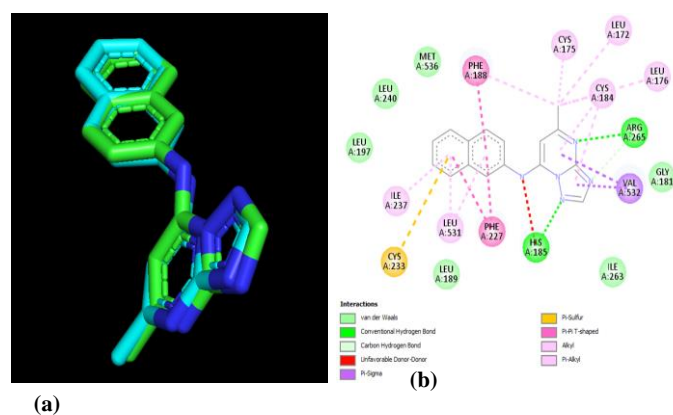


Figure 4: (a) superimposition of the native DSM1 before docking with the docking pose with an estimated rmsd of 0.15 Å (a validation of the docking protocol); (b) The 2D diagram of DSM1 bound to *Pf*DHODH showing the interactions with neighboring amino acid residues.

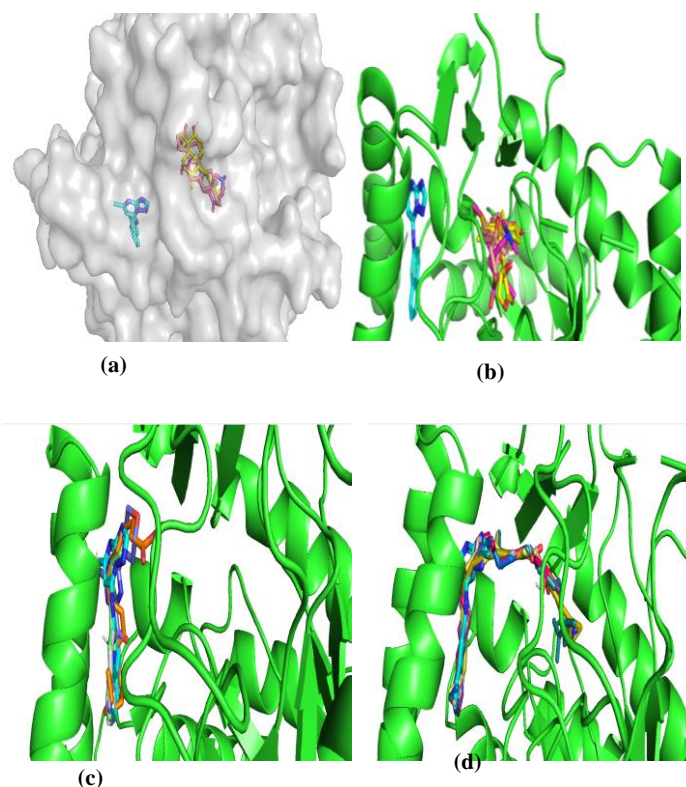


Figure 5: (a) DSM1 (cyan) bound at allosteric site deep within the protein (surface rendition) and compounds (multiple colour for different ligands) bound at active site at a different region within the protein; (b) The other compounds bound at the active site (in the cluster of cartoon rendering) include (i) MET24_671 (Magenta), (ii) MET25_998 (yellow) and (iii) MET28_688 (brown); (c) The other compounds bound at the allosteric site along with DSM1 include (iv) DCM27_869 (Grey), (v) MET25_300 (indigo), (vi) MET26_502 (orange); (vii) EA24_614 (green); (d) Compounds that bound to both binding pockets passing through the groove that connects the two domains. All clustered in multiple colours apart from DSM1 (cyan) and these include, DCM27_669, EA19_464, EA22_622, MET21_598, MET22_050 and MET23_566.

Authors' Declaration

The authors hereby declare that the work presented in this article is original and that any liability for claims relating to the content of this article will be borne by them.

Acknowledgements

The authors acknowledge the contributions of Dr. Oyebamiji A. Kolawole (Industrial Chemistry Programme, Bowen University, Iwo, Osun State) towards the success of this study.

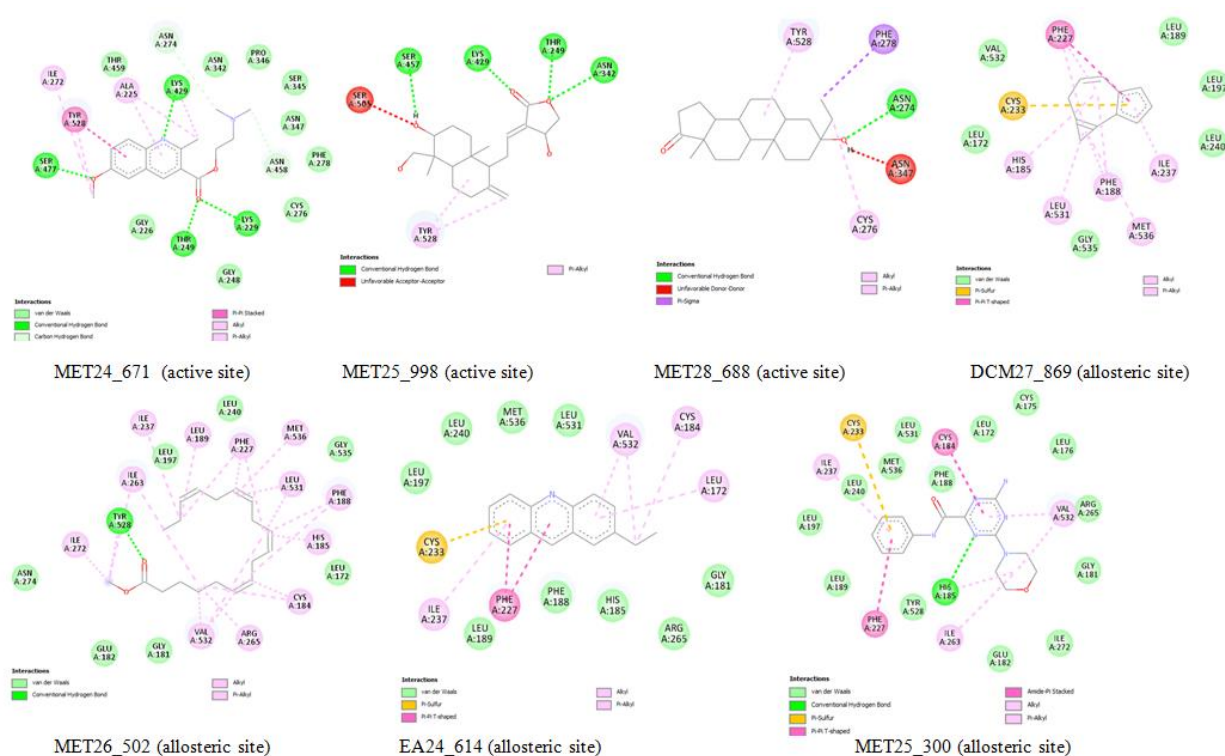


Figure 6: The binding poses of compounds that bound to allosteric site (inhibitor binding domain) and active site in 2D

References

- Jarukamjorn K, Nemoto N. Pharmacological Aspects of *Andrographis paniculata* on Health and Its Major Diterpenoid Constituent Andrographolide. *J. Health Sci.* 2008; 54(4): 370-381.
- Okhuarobo A, Falodun JE, Erharuyi O, Imieje V, Falodun A, Langer P. Harnessing the medicinal properties of *Andrographis paniculata* for diseases and beyond: a review of its phytochemistry and pharmacology. *Asian Pac J Trop Dis* 2014; 4(3):213-222.
- Ukpanukpong RU, Bassey SO, Akindahunsi DO, Omang WA, Ugor JA. Antidiarrheal and Antihepatic Effect of *Andrographis paniculata* Leaf Extract on Castor Oil Induced Diarrhea in Wistar Rats. *The Pharm. chem. j.* 2018; 5(1): 62-76.
- <https://www.sciencedirect.com/topics/agricultural-and-biologicalsciences/phytochemical>. [online]. [cited 2023 May 3].
- Ikotun AA, Babajide EE, Omolekan TO, Ajaelu CJ. In vitro Antioxidant Activities of Some Re(I) Metal Carbonyls Synthesized from Isatin Derivatives. *Trop. J. Nat. Prod. Res.* 2022; 6(10): 1723-1726.
- Afolayan FI, Ijidakirno OD. In silico antiparasitic investigation of compounds derived from *Andrographis paniculata* on some parasites validated drug targets. *Afr. J. Bio. Sci.* 2021; 3(3): 93-110.
- Mishra SK, Sangwan NS, Sangwan RS. *Andrographis paniculata* (Kalmegh): A Review. *Phcog. Rev* 2007; 1(283): 283-298.
- Zeng B, Wei A, Zhou Q, Yuan M, Lei K, Liu Y, Song J, Guo L, Ye Q. Andrographolide: A review of its pharmacology, pharmacokinetics, toxicity and clinical trials and pharmaceutical researches. *Phytother Res.* 2022; 36(1): 336-364.
- Hossain S, Urbi Z, Karuniawati H, Mohiuddin, RB, Moh Qrimida, A, Allzrag AMM, Ming LC, Pagano E, Capasso R. *Andrographis paniculata* (Burm. f.) Wall. ex Nees: An Updated Review of Phytochemistry, Antimicrobial Pharmacology, and Clinical Safety and Efficacy. *Life* 2021; 11(4): 348.
- Kumar S, Singh, B, Bajpai, V. *Andrographis paniculata* (Burm.f.) Nees: Traditional uses, phytochemistry, pharmacological properties and quality control/quality assurance. *J Ethnopharmacol.* 2021; 275: 114054.
- Jayakumar T, Hsieh CY, Lee JJ, Sheu JR. Experimental and Clinical Pharmacology of *Andrographis paniculata* and Its Major Bioactive Phytoconstituent Andrographolide. *Evid Based Complement Alternat Med.* 2013; 2013: 846740.
- White NJ. Antimalarial drug resistance. *J Clin Invest.* 2004; 113(8): 1084-1092.
- Wicht KJ, Mok S, Fidock DA. Molecular Mechanisms of Drug Resistance in *Plasmodium falciparum* Malaria. *Annu Rev Microbiol.* 2020; 74: 431-454.
- Roux AT, Maharaj L, Oyegoke O, Akoniyan OP, Adeleke MA, Maharaj R and Okpeku M. Chloroquine and Sulfadoxine-Primethamine Resistance in Sub-Saharan Africa-A Review. *Front. Genet.* 2021; 12: 668574.
- Zhu L, van der Pluijm RW, Kucharski M, Nayak S, Tripathi J, White NJ, Day NPJ, Faiz A, Phyo AP, Amaratunga C, Lek D, Ashley EA, Nosten F, Smithuis F, Ginsburg H, von Seidlein L, Lin K, Imwong M, Chotivanich K, Mayxay M, Dhorda M, Nguyen HC, Nguyen TNT, Miotto O, Newton PN, Jittamala P, Tripura R, Pukrittayakamee S, Peto TJ, Hien TT, Dondorp AM, Bozdech Z. Artemisinin resistance in the malaria parasite, *Plasmodium falciparum*, originates from its initial transcriptional response. *Commun Biol.* 2022; 5(1): 274.
- Ward KE, Fidock DA, Bridgford JL. *Plasmodium falciparum* resistance to artemisinin-based combination therapies. *Curr Opin Microbiol.* 2022; 69: 102193.
- da Silva C, Matias D, Dias B, Cancio B, Silva M, Viegas R, Chivale N, Luis S, Salvador C, Duarte D, Arnaldo P, Enosse S, Nogueira F. Anti-malarial resistance in Mozambique: Absence of *Plasmodium falciparum* Kelch 13

- (K13) propeller domain polymorphisms associated with resistance to artemisinins. *Malar J.* 2023; 22(1): 160.
18. Hyde JE. Exploring the folate pathway in *Plasmodium falciparum*. *Acta Trop.* 2005; 94(3): 191-206.
 19. Yuthavong Y. Antifolate Drugs. In: Hommel M, Kresmsner P (eds) *Encyclopedia of Malaria*. Springer, New York, NY; 2013. Vol 1-12.
 20. Herraiz T, Guillén H, González-Peña D, Arán VJ. Antimalarial Quinoline Drugs Inhibit β -Hematin and Increase Free Hemin Catalyzing Peroxidative Reactions and Inhibition of Cysteine Proteases. *Sci Rep.* 2019; 9(1): 15398.
 21. Kapishnikov S, Staalsø T, Yang Y, Lee J, Pérez-Berná AJ, Pereiro E, Yang Y, Werner S, Guttmann P, Leiserowitz L, Als-Nielsen J. Mode of action of quinoline antimalarial drugs in red blood cells infected by *Plasmodium falciparum* revealed in vivo. *Proc Natl Acad Sci U S A.* 2019; 116(46): 22946-22952.
 22. O'Neill, PM, Barton VE, Ward SA. The Molecular Mechanism of Action of Artemisinin—The Debate Continues. *Molecules* 2010; 15(3): 1705-1721.
 23. Meshnick SR. Artemisinin antimalarials: mechanisms of action and resistance. *Med Trop (Mars).* 1998; 58(3 Suppl): 13-17.
 24. Hasan MA, Mazumder MH, Chowdhury AS, Datta A, Khan MA. Molecular-docking study of malaria drug target enzyme transketolase in *Plasmodium falciparum* 3D7 portends the novel approach to its treatment. *Source Code Biol Med.* 2015; 10: 7.
 25. Boateng RA, Tastan Bishop Ö, Musyoka TM. Characterisation of plasmodial transketolases and identification of potential inhibitors: an in silico study. *Malar J.* 2020; 19(1): 442.
 26. Cassera MB, Zhang Y, Hazleton KZ, Schramm VL. Purine and pyrimidine pathways as targets in *Plasmodium falciparum*. *Curr Top Med Chem.* 2011; 11(16): 2103-2115.
 27. Frame IJ, Deniskin R, Arora A, Akabas MH. Purine import into malaria parasites as a target for antimalarial drug development. *Ann N Y Acad Sci.* 2015; 1342(1): 19-28.
 28. Hoelz LV, Calil FA, Nonato MC, Pinheiro LC, Boechat N. *Plasmodium falciparum* dihydroorotate dehydrogenase: a drug target against malaria. *Future Med Chem.* 2018; 10(15): 1853-1874.
 29. Phillips MA, Rathod PK. *Plasmodium* dihydroorotate dehydrogenase: a promising target for novel anti-malarial chemotherapy. *Infect Disord Drug Targets.* 2010; 10(3): 226-239.
 30. Hyde JE. Targeting purine and pyrimidine metabolism in human apicomplexan parasites. *Curr Drug Targets* 2007; 8(1): 31-47.
 31. Phillips MA, Rathod PK, Rueckle T, Matthews D, Burrows JN, Charman SA. Medicinal Chemistry Case History: Discovery of the Dihydroorotate Dehydrogenase Inhibitor DSM265 as an Antimalarial Drug Candidate. In Chackalamannil S, Rotella D, Ward SE, editors, *Comprehensive Medicinal Chemistry III: Case Histories in Recent Drug Discovery*. 3 ed. Vol. 8. Amsterdam The Netherlands: Elsevier. 2017. p. 544-557. (Reference Module in Chemistry, Molecular Sciences and Chemical Engineering; 3).
 32. Xu Y, Jiang H. Potential treatment of COVID-19 by inhibitors of human dihydroorotate dehydrogenase. *Protein cell.* 2020; 11(10): 699-702.
 33. Faboro EO, Wei L, Liang S, McDonald AG, Obafemi CA. Phytochemical Analyzes from the Leaves of *Bryophyllum pinnatum*. *European j. med. plants* 2016; 14(3): 1-10.
 34. O'Boyle NM, Banck M, James CA, Morley C, Vandermeersch T, Hutchison GR. Open Babel: An open chemical toolbox. *J Cheminform.* 2011; 3(33).
 35. Trott O, Olson AJ. AutoDock Vina: improving the speed and accuracy of docking with a new scoring function, efficient optimization, and multithreading. *J Comput Chem.* 2010; 31(2): 455-461.
 36. The PyMOL Graphics System, Version 2.0 Schrödinger, LLC. [Online]. 2023 [cited 2023 April 15]. Available from: Support | pymol.org.
 37. Ouzebila D, Ourhriss N, Fadare OA, Belghiti ME, El Abdallaoui HE, Zeroual A. Efficient Synthesis of Acyclic Nucleosides by N-Alkylation Using K₂CO₃ Supported with Natural Phosphate (K₂CO₃@NP) as Catalyst and Docking Study Against VIH. *Chem Afri.* 2022; 6(1): 881-890.
 38. Xiong G, Wu Z, Yi J, Fu L, Yang Z, Hsieh C, Yin M, Zeng X, Wu C, Lu A, Chen X, Hou T, Cao D. ADMETlab 2.0: an integrated online platform for accurate and comprehensive predictions of ADMET properties. *Nucleic acids Res.* 2021; 49(W1): W5-W14.
 39. Kyei LK, Gasu EN, Ampomah GB, Mensah JO, Borquaye LS. An In Silico Study of the Interactions of Alkaloids from *Cryptolepis sanguinolenta* with *Plasmodium falciparum* Dihydrofolate Reductase and Dihydroorotate Dehydrogenase. *J Chem.* 2022; 2022.
 40. Mishra K, Dash AP, Dey N. Andrographolide: A Novel Antimalarial Diterpene Lactone Compound from *Andrographis paniculata* and Its Interaction with Curcumin and Artesunate. *J Trop Med.* 2011; 2011: 579518.
 41. Kim SK, Karadeniz F. Biological importance and applications of squalene and squalane. *Adv Food Nut Res.* 2012; 65: 223-233.
 42. Huang ZR, Lin YK, Fang JY. Biological and pharmacological activities of squalene and related compounds: potential uses in cosmetic dermatology. *Molecules.* 2009; 14(1): 540-54.
 43. Islam MT, Ali ES, Uddin SJ, Shaw S, Islam MA, Ahmed MI, Chandra Shill M, Karmakar UK, Yarla NS, Khan IN, Billah MM, Pieczynska MD, Zengin G, Malainer C, Nicoletti F, Gulei D, Berindan-Neagoe I, Apostolov A, Banach M, Yeung AWK, El-Demerdash A, Xiao J, Dey P, Yele S, Józwick A, Strzałkowska N, Marchewka J, Rengasamy KRR, Horbańczuk J, Kamal MA, Mubarak MS, Mishra SK, Shilpi JA, Atanasov AG. *Phytol*: A review of biomedical activities. *Food Chem Toxicol.* 2018; 121: 82-94.
 44. Bickerton GR, Paolini GV, Besnard J, Muresan S, Hopkins AL. Quantifying the chemical beauty of drugs. *Nat Chem.* 2012; 4(2): 90-98.